Multimodal travelling wave MRI with two coaxial modules

Stefan Alt[1], Reiner Umathum[1], Wolfhard Semmler[1], and Michael Bock[1,2]

[1]Dept. of Medical Physics in Radiology, German Cancer Research Center (DKFZ), Heidelberg, Germany, [2]Radiology - Medical Physics, University Hospital Freiburg, Freiburg, Germany

INTRODUCTION

Various travelling wave (TW-MRI) [1] approaches have been suggested for high-field MRI systems ($B_0 \geq 7T$) to provide a homogeneous RF excitation similar to a body coil. Among these, the symmetric coaxial setup [2] is able to focus the RF exposition to the actual imaging area. Its basic coaxial propagation mode TEM (transverse electromagnetic) has no cut-off frequency, but the field distribution has an undesirable B_1^+ void along the central axis of propagation. To overcome this limitation we propose the use of 2 coaxial modules (Fig. 1), that can be shifted along the magnet bore to define an imaging area (FOV), to bring the feed points closer the imaging area. In this way, propagating (e.g. TEM, TE11) as well as evanescent higher-order (e.g. TE21) modes can be excited and used for spin excitation, which presents an advantage over previous multimodal TW-MRI approaches [3-5]. Simulation results of a setup with 8 feed points, driven with 5 different settings, are shown and the resulting B_1^+ and SAR field distributions are analyzed.

MATERIAL & METHODS

The performance of the suggested coaxial module setup (Fig. 1a) was assessed using FDTD simulations (SemcadX 14, Speag AG, Zuerich, Switzerland). The setup is loaded with the virtual family model "Ella" [6], so that the imaging area encloses the thorax and abdomen of the model. Magnet bore (length: 3m) and module surfaces were simulated to be perfectly conductive, and transition caps were introduced that closely fit the human model. The setup is driven by 8 current sources ($\alpha_1, \cdots, \alpha_4, \beta_1, .., \beta_4$) in radial orientation at the left module, while the right module is matched to act as a reflection-free termination. Here, the termination was simulated with an absorbing boundary condition. Both modules can be used for signal reception if no local Rx hardware is used. Each simulation was run with harmonic excitation at the 7T Larmor frequency of 297MHz and a discretization grid of 12 million cells. A current of 1 A was applied to each active source, and phase delays were set to excite different modes of propagation (see Tab. 1).

RESULTS AND DISCUSSION

Simulations showed that the TEM and TE (transverse electric) modes are maintained throughout the imaging area near the magnet bore wall, but the fields are distorted near and within the phantom, thus creating B1+ distributions (Fig. 2), which do not resemble the originally excited mode patterns of an empty coaxial waveguide. Even in TEM mode, which should not contain any B_z components, only approx. 50% of the total B_1 within the body is left in the transverse plane and is usable for spin excitation. As expected, this is further reduced to 30/45% for TE11/TE21. While transmission efficiencies up to 10 $\mu T/kW^{1/2}$ are reached in the arms and in distal body regions, B_1^+ decreases significantly to the center of the body. This results in mean transmission efficiencies of ≤ 3.2 $\mu T/kW^{1/2}$, which is inferior to resonant structures, but similar to other travelling wave approaches. Spin excitation as well as SAR exposition are mainly restricted to the region between the coaxial modules (FOV, see Fig. 3). As all tested modes lack penetration depth, a homogeneous spin excitation by B1-shimming (i.e. superposition of diverse B_1^+ distributions) over the complete FOV cannot be realized, but is feasible for a smaller target organ. Furthermore, the non-rotating modes (TE11, TE21) can be excited in any tilted orientation to create more diverse B_1^+ distributions, or additional feed points can be used to excite higher order modes of propagation.

CONCLUSION

The multimodal setup shown here can complement the original coaxial TW- MRI approach by exciting higher order modes, which result in various B_1^+ distributions and allow for a limited B_1-shimming by superposition. As the feed points are placed near the imaging area, even evanescent modes can be utilized. RF focusing to the imaging area is maintained, but transmission efficiencies may be too low for pulse sequences requiring high flip-angles or imaging of medial regions. The addition of more higher-order modes and B_1-shimming by superposition will be covered in further studies.

REFERENCES

[1] Brunner et al. Nature, **457**(7232):971-972 (2009) [2] Alt et al., Mag Res Med (pub. ahead of print), DOI: 10.1002/mrm.23069 [3] Brunner et al, Mag Res Med, **66**:290–300 (2011) [4] Alt et al, ISMRM 2010:623 [5] Andreychenko et al, ISMRM 2011:624 [6] http://www.itis.ethz.ch/index/index_humanmodels.html
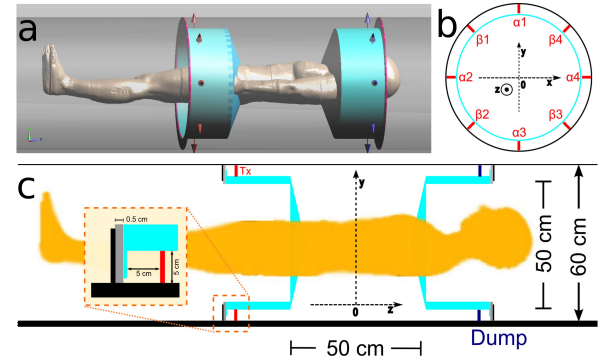
Figure 1: (a) 3D-rendering of the simulation setup. The travelling waves are excited by the edge sources in the left module (red arrows), pass through the central imaging area and are dissipated in the module to the right. (b) Source distribution. (c) Schematic view of the coaxial modules (turquoise) placed within the magnet bore (black).

	α1	α2	α3	α4	β1	β2	β3	β4
1:TEM	0°	0°	0°	0°	-	-	-	-
2:TE11	0°	-	180°	-	-	-	-	-
3:TE21	0°	180°	0°	180°	-	-	-	-
4:rotTE11	0°	90°	180°	270°	-	-	-	-
5:rotTE21	0°	180°	0°	180°	90°	270°	90°	270°

Table 1: Phase delays applied to the sources depicted in Fig. 1b to create 5 different propagation modes. In 4 and 5, two TE11/TE21 excitations are overlaid quadrature-like to create a TE11/TE21 distribution rotating around the z- axis, respectively.
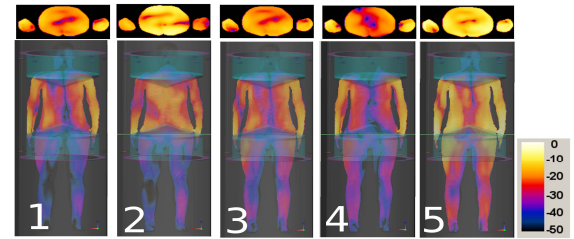

Figure 2: B_1^+ distributions (dB-scaled to $10\mu T/kW^{1/2}$) in transverse and coronal slices through the center for all 5 modes.
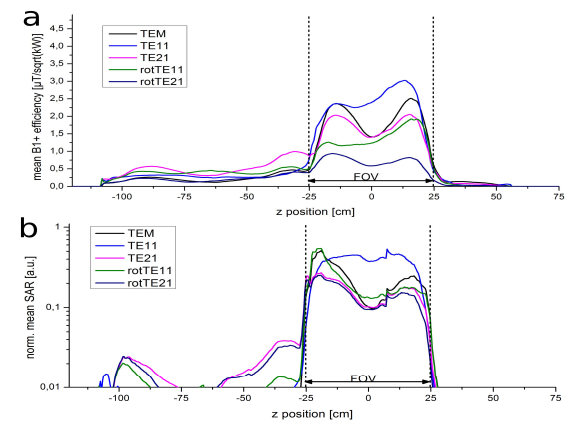

Figure 3: Mean transmission efficiency and SAR distributions, averaged within transverse slices along the length of the phantom.